Absorption and Attenuation in Soft Tissues II—Experimental Results

MARK E. LYONS AND KEVIN J. PARKER, SENIOR MEMBER, IEEE

Abstract—**To determine the relative contributions of ultrasonic loss mechanisms in tissues, independent measurements of total attenuation and local absorption were obtained at discrete frequencies within the range of medical diagnostic equipment, 1–13 MHz. Automation techniques were applied to aspects of experimentation where extensive averaging or curve fitting could be used to improve accuracy [1]. New approaches were also implemented to calibrate focused beams for use in pulse-decay absorption measurements which covered a wider frequency range, utilizing smaller sample volumes than were previously practical. These approaches enable comparisons of the magnitude and frequency dependence of attenuation and absorption in biological media, and permit some inferences to be made as to the relative contribution of scattering to total attenuation. The results of studies on agar-gelatin phantoms, calf liver, and collagenous pig liver indicate that absorption comprises 90–100 percent of total attenuation in these materials. Studies on bovine brain matter and leg muscle are less definitive because complications include the inhomogeneous grey and white matter composition of brain, and fiber anisotropy in muscle. However, average results from these tissues also show a major contribution of absorption to attenuation.**

I. Introduction

THE ultrasonic attenuation, absorption, and scattering coefficients of tissues are not well characterized despite their importance to diagnostic imaging, therapeutic applications, and tissue characterization. The relative contributions of scattering and absorption to total attenuation are of particular relevance to models of tissue–ultrasound interaction. Only recently were capabilities developed for the direct measurement of total scattered power [2], so previous comparisons typically determined attenuation and/or absorption coefficients, inferring indirectly the contribution of scattering to total attenuation. Pauly and Schwan [3] reported 30-percent lower attenuation in homogenized liver compared to whole liver. Presumably the destruction of scattering structures resulted in the lower attenuation. Other attenuation and absorption values from the literature [4]–[7] can lead to the conclusion that attenuation coefficients are a factor of 2 or more higher than absorption coefficients in mammalian tissues, implying substantial contributions of scattering to total attenuation. However, in the 1970's sources of error were described that tended to artificially increase attenuation estimates (phase cancellation error [8], bubbles [9]) and decrease absorption estimates (heat conduction from narrow beamwidths [10]). Also, the pulse decay technique [11], [12] was developed to overcome some errors and limitations of the rate of heating absorption method.

Taken as a whole, these developments suggest that attenuation and absorption coefficients may converge as newer approaches are implemented. The measurements of Campbell and Waag [2] on calf liver produced an estimate of 2 percent contribution of scattering to total attenuation over a frequency range of 3–7 MHz. Parker's data [13] on bovine liver showed no statistical difference between absorption and attenuation at 1 and 3 MHz, although a difference of greater than 10 percent was found at 5 MHz. A re-evaluation of homogenization experiments failed to reproduce the Pauly and Schwan result, and instead showed no significant difference between attenuation of whole and homogenized liver [14], [17]. This paper provides independent estimates of attenuation and absorption for an agar-gelatin phantom, calf liver, pig liver, bovine brain, and bovine leg muscle tissue. The results show that absorption is the dominant loss mechanism of ultrasound propagating through soft tissues.

II. Methods and Materials

A. Sample Preparation

All animal tissues were obtained from a commercial slaughterhouse within 0–2 h *post mortem*. Whole organs were placed immediately in chilled, degassed saline and stored at 4°C for experiments performed 2–24 h *post mortem*. All subsequent tissue handling was performed underwater in chilled saline. Some samples were frozen in saline and thawed for later use. Experiments showed no difference between properties of fresh and frozen-thawed samples when bubbles are eliminated as a source of error [9], [13]. Surgical blades were used to cut sections with nearly parallel faces, and pill-box shaped holders with thin plastic film faces in tension were used to enforce sample geometry. All ultrasonic measurements were performed at room temperature 20–22° in degassed demineralized water. Sample thickness was measured with both a micrometer and pulse-echo examination of the specimen using an assumed velocity of 1540 m/s. For all samples (except brain) attenuation and absorption measurements were obtained on the same day, using identical samples or adjacent sections from the same organ.

Paper received Jaunary 20, 1987; revised May 6, 1987. This work supported by NSF grant ECE-8643973.

The authors are with the Department of Electrical Engineering, University of Rochester, Rochester, NY 14627.

IEEE Log Number 8719106.

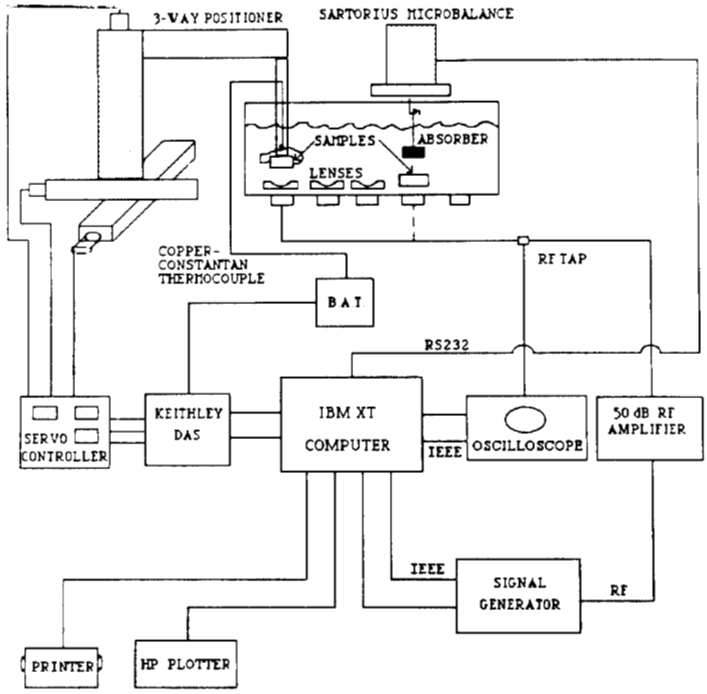

Fig. 1. Experimental apparatus. Measurements of pulse-decay absorption use removable Lucite lenses to produce focused fields; temperature measurements are obtained from embedded thermocouples. Attenuation measurements employ collimated unfocused beams with radiation force measured by electronic microbalance.

B. Equipment

The automated experimental apparatus is shown in Fig. 1. An XT "personal computer" (IBM) controls a data-acquisition system (Keithley 500 series D.A.S.) which communicates with precision x–y–z positioning axes (Velmex B6000 Unislide), and a thermocouple preamp (Bailey Instruments B.A.T.-4). The *XT* interfaces with a digitizing oscilloscope (Tektronix 7D20) and radiofrequency (RF) function generator (Tektronix FG5010) via an IEEE–GPIB interface. A precision microbalance (Sartorius 1801 MP8) is used for radiation force measurements, and outputs data to the XT under RS-232 protocol. The overall data acquisition, analysis, and display are handled by programs written in the ASYST (McMillan Software) operating system.

The acoustic fields are generated by 5 ceramic 1-in diameter transducers. The fundamental and odd harmonics provide 15 discrete frequencies between 0.5 and 13 MHz. Removable Lucite lenses are used to focus at 8 cm in pulse-decay experiments. Fixed wall absorbers and floating irregular absorbers of RTV and natural rubbers are used to produce anechoic conditions.

C. Attenuation Measurements

Radiation force insertion loss measurements are employed to determine amplitude attenuation coefficients under continuous wave (CW) irradiation, with uncertainties on the order of 4–10 percent [3]. Under computer control the power measurements with and without samples present are obtained by averaging 15 consecutive microelectronic balance readings (0.1-mg resolution) before and during irradiation at preselected frequencies and power levels low enough to avoid nonlinear effects. Samples are placed in and out of the field for up to ten repeat measurements. The statistics of radiation force with and without sample present are calculated, permitting estimation of attenuation coefficient with error bars [1].

D. Pulse-Decay Absorption

Embedded calibrated copper–constantan thermocouples are used to measure temperature history of CW irradiated tissue, yielding absorption coefficients with accuracies of 10 percent [1], [11], [12].

Full use was made of the integral–differential relationships between pulse-decay and rate-of-heating experiments; the latter is advantageous under conditions where a limit on intensity (because of the onset of nonlinear shock, for example) produces inadequate heating during the pulse decay. Direct analysis of rate-of-heating curves is impractical because no analytical expressions are available for curve fits to these data, and because the viscous heating produces an additive constant of unknown amplitude that further complicates curve fit procedures. Since this relationship has not previously been examined in detail, a short description is given below.

The mathematical description of the ideal intensity impulse function used in the pulse-decay experiment can be described using the delta function:

$$I(t)_{PD} = I_0 \delta(t). \tag{1}$$

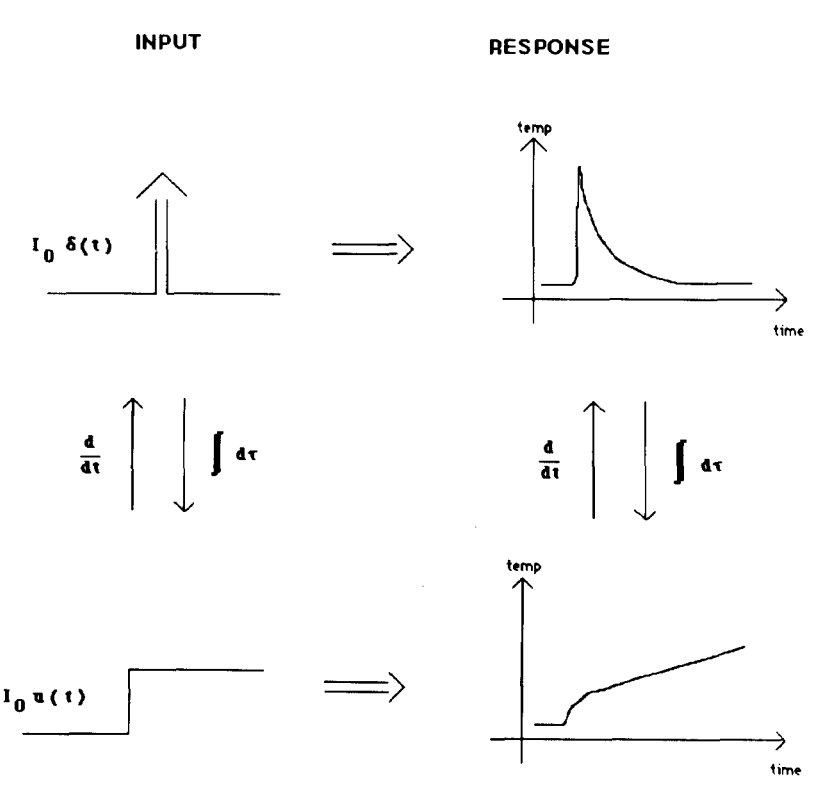

Fig. 2. Integral-differential relation exists between intensity impulse and step functions (inputs), and therefore similar relationship exists between pulse-decay and rate-of-heating temperature histories (outputs).

Similarly, the intensity function used in the rate-of-heating experiment is described with the aid of the unit step function:

$$I(t)_{RH} = I_0 u(t). \tag{2}$$

The relationship between the two intensity functions may be described using linear system theory:

$$\frac{\partial}{\partial t}\left[I_0 u(t)\right] = I_0 \delta(t) \tag{3}$$

$$\int_{-\infty}^{t} \left[I_0 \delta(\tau)\right] d\tau = I_0 u(t). \tag{4}$$

Because these inputs to a linear system bear an integral-differential relation, the corresponding outputs (temperature histories) of a linear system will also have an integral-differential relationship as shown in Fig. 2.

In reality the impulse function used in the pulse-decay experiment is not ideal:

$$I(t) = \begin{cases} I_0 s; & 0 \le t \le \Delta t \\ 0 & \text{otherwise} \end{cases} \tag{5}$$

where s is an intensity scale factor required because of the limited range of the recording instruments. The finite on-time Δt can be short enough (0.01 s) to be thermally impulsive, while long enough to be generated by a quasi-continuous-wave (CW) tone burst at frequency f_0. The integral-differential relationship is modified slightly to account for the nonideal impulse function

$$T_{PD} = s\Delta t \frac{\partial}{\partial t} T_{RH} \tag{6}$$

$$T_{RH} = \frac{1}{s\Delta t} \int_0^t T_{PD}\, d\tau. \tag{7}$$

Fig. 3 is an experimental comparison of the integral-differential relationship where agreement is within experimental error. Thus, as an alternative to doing an actual pulse decay, one can do a rate-of-heating experiment (at a reduced intensity level), then differentiate the data (after filtering out high-frequency noise) and analyze it as a pulse decay. The effects of viscous heating are minimized by eliminating the first 0–1.5 s of data from the curve fit procedure [11], [12].

Each experiment began with 51-μm thermocouple placement at a measured distance (usually 1–3 mm) below the surface of the sample in a surgical incision. The sample was placed in a holder and sealed from the external environment with acoustic windows. The holder was attached to the three-way positioner and centered over the transducer–lens combination. Several scans in each of the three axes were performed until the junction of the thermocouple was in the focus of the ultrasonic beam. Once this was accomplished, a radial scan (101 points) was made and stored to record the beam shape and calibrate intensity. When the scan was completed, the sample was automatically returned to the focus. Next the pulse-decay

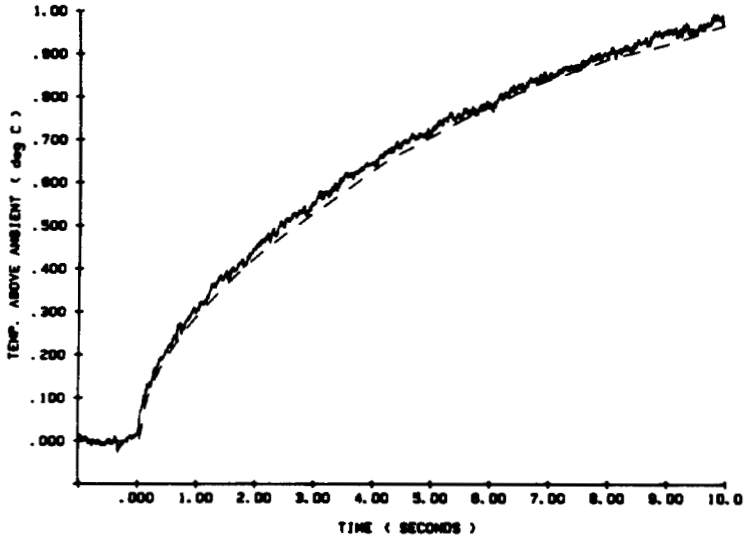

(a)

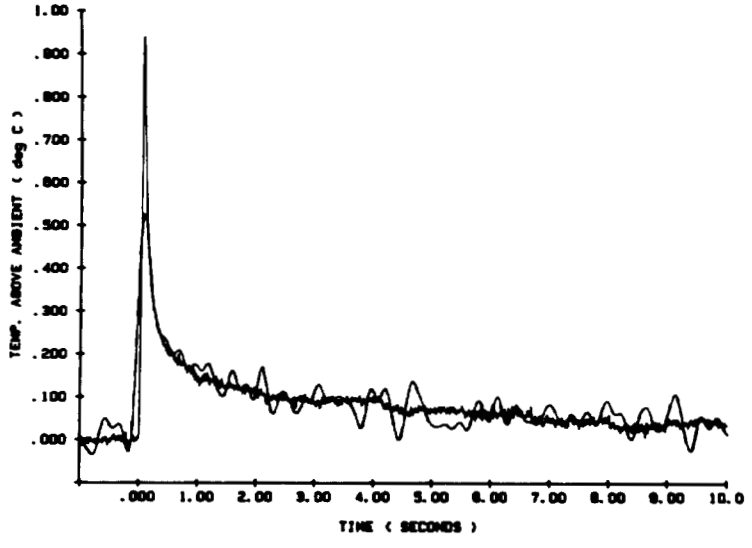

(b)

Fig. 3. Experimental verification of integral–differential relation between rate of heating and pulse decay, as measured at 1-mm depth in absorbing rubber. a) Measured 10-s rate of heating (solid line) and time integral of pulse decay. b) 10-s pulse decay (thick solid line) and time derivative of corresponding rate of heating (thin solid line).

experiments (8–9 per frequency) were conducted. At each frequency, three experiments were conducted at radius $r = 0$, three at $r = [\beta]^{1/2}$, and three at $r = 2 * [\beta]^{1/2}$, where $\beta^{1/2}$ is the Gaussian beam width. An exception is that no far off-axis measurements ($r = 2 * [\beta]^{1/2}$) were taken for the largest beamwidths at 1 and 2 MHz. For each experiment a value of alpha was derived and all the values at a given frequency were averaged. Figs. 4(a)–(c) show the typical experimental results in calf liver with the theoretical curve fit of the model (dashed lines) for 5-MHz insonation, and different values of r. A noticeable feature of these graphs is the changes in shape and drop in magnitude of the curves with different radial positions. Another noticeable feature of the curves is the low-frequency ripple in the experimental data, which results from numerical differentiation of rate-of-heating data. As long as this unfiltered noise is zero mean, it should not significantly affect the outcome of the analysis. No significant differences were found between measurements taken on axis ($r = 0$) and off axis ($r = \beta^{1/2}$ or $2 * \beta^{1/2}$), with a typical scatter in data of about 10 percent.

Before or after the absorption measurements were obtained, the total power emitter by the transducer and transmitted through the lens was measured using the radiation force technique.

The pulse-decay curve fit of peak temperature, the intensity profile, and power measurements were used to calculate an initial estimate of absorption coefficient. An iterative procedure was then used to correct for the change in intensity with sample depth to the level of the thermocouple, resulting in absorption coefficients higher than their initial estimates.

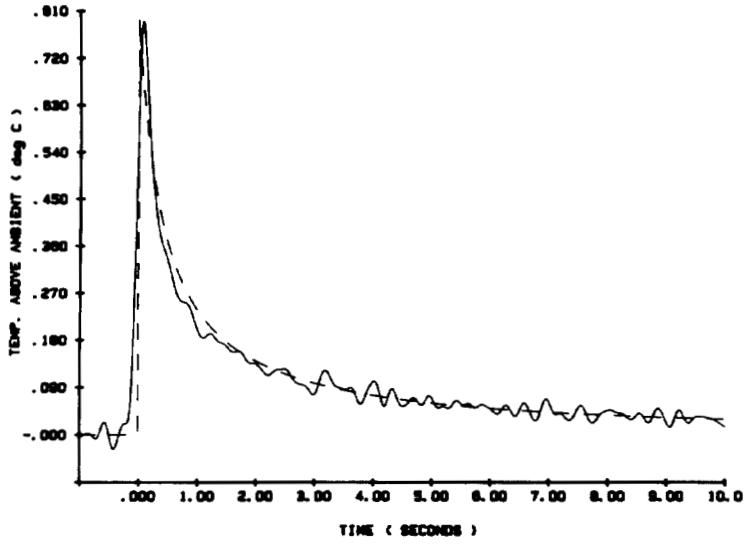

(a)

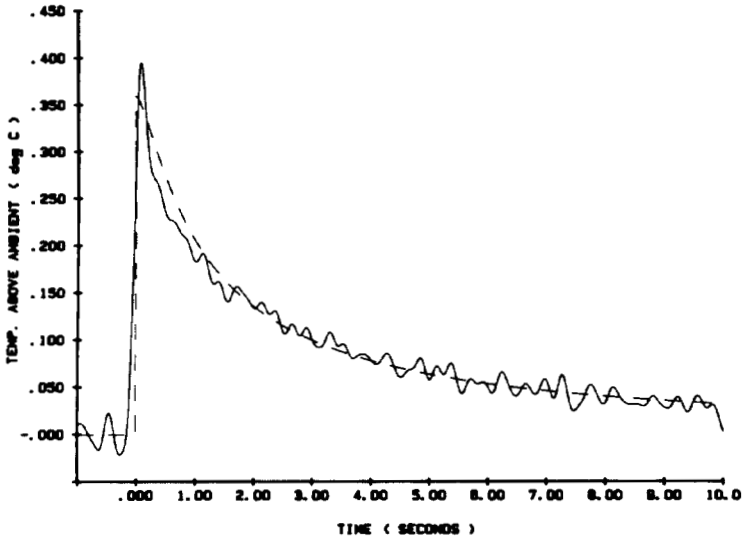

(b)

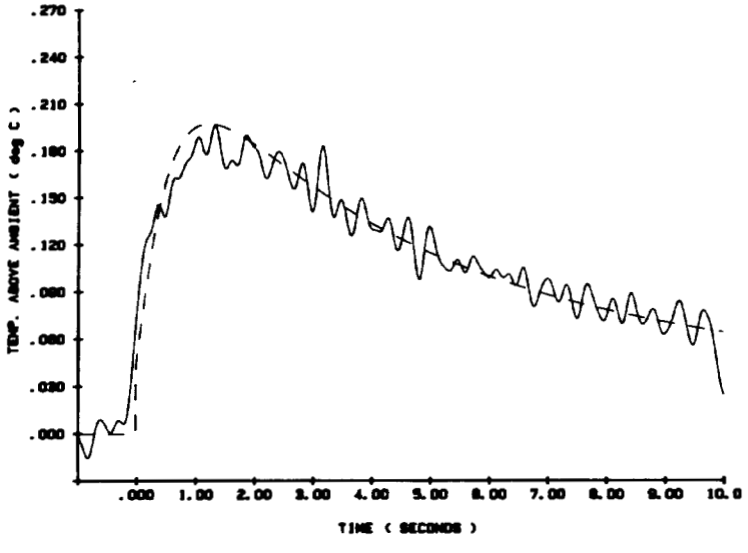

(c)

Fig. 4. Typical experimental results and theoretical curves fit to pulse-decay experiments in calf liver at 5 MHz, for on- and off-axis positions. (a) $r = 0$. (b) $r = \beta^{1/2}$. (c) $r = 2 * \beta^{1/2}$.

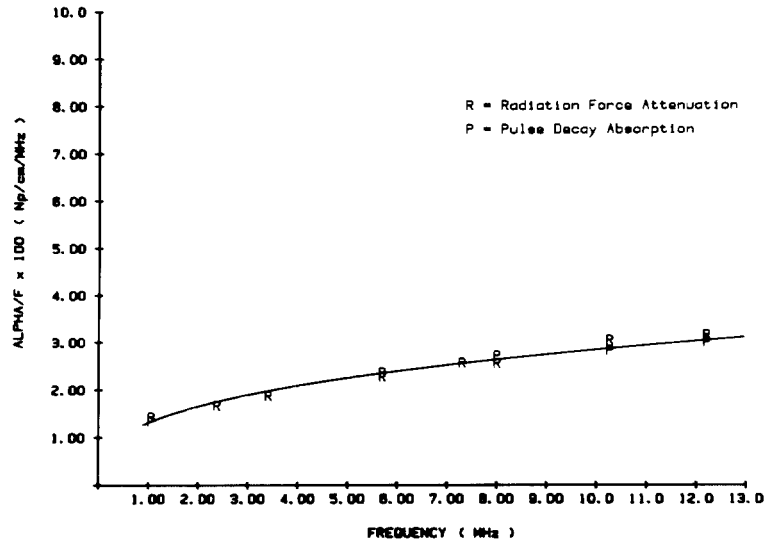

Fig. 5. Absorption (P) and attenuation (A) coefficients divided by frequency ($100 \times$ Np/cm · MHz) versus frequency for homogeneous, nonscattering agar-gelatin phantom. Solid lines are curve fits of data to power law functions, which appear as single line because of overlap.

III. Results

A. Verification Using a Known Phantom

In a homogeneous medium with no scattering, experimental procedures should find no difference between absorption and attenuation measurements. Accordingly, a phantom was constructed with low reflection coefficient (good impedance match to water), similar thermal properties to those of tissues, and reasonable attenuation to ensure adequate signal-to-noise ratio at moderate intensities. A mixture of 5-percent agar and 5-percent gelatin dissolved in degassed distilled water was found to produce a useful homogeneous solid phantom. Fig. 5 is a summary of four experiments performed on this phantom, with power-law curves fit to attenuation and absorption data. The two are sufficiently close as to be indistinguishable. Table I gives the least-squares-error power-law fit for all absorption and attenuation data from the phantom and tissues, where the correlation coefficient (goodness of fit) is greater than 0.95 in all cases.

This excellent agreement of the two independent measurements demonstrates that the pulse-decay model is experimentally valid over a broad frequency range, even at high frequencies with submillimeter focal beamwidths. Also it shows that the method chosen to determine absolute peak intensity is valid [1]. Thus the experimental techniques appear adequate for correctly inferring a near-zero contribution from scattering in this case.

B. Calf Liver

Fig. 6 is a summary of the experimental data collected from 15 liver samples (fresh and frozen) from six whole organs. The experiments for absorption and attenuation of a given sample were always done on the same day using adjacent pieces of the same liver. However, the order of which was done first (absorption or attenuation) was varied so as not to introduce a systematic error. Also, when doing the absorption and attenuation measurements the order of frequencies was varied from sample to sample.

TABLE I
Power Law Fit of Attenuation and Absorption (Np/cm)

Sample Name	Radiation Force Attenuation	Pulse Decay Absorption
Agar + gelatin	$\alpha = 0.013 f^{1.34}$	$\alpha = 0.013 f^{1.33}$
Calf liver	$\alpha = 0.032 f^{1.30}$	$\alpha = 0.030 f^{1.29}$
Pig liver	$\alpha = 0.034 f^{1.32}$	$\alpha = 0.032 f^{1.30}$
White brain	α not measured	$\alpha = 0.064 f^{1.27}$
Grey brain	α not measured	$\alpha = 0.012 f^{1.21}$
White + grey mixture	$\alpha = 0.040 f^{1.17}$	α not measured

Fig. 6 shows a power-law curve fit (least squares error) to both attenuation ($\alpha/f = 0.032\ f^{0.30}$) and absorption ($\alpha/f = 0.030\ f^{0.29}$) coefficients. Dunn *et al.* [15] reported attenuation values in the range 0.07–0.13 Np/cm at 1 MHz for calf liver, which are high compared to our values. Goss *et al.* [6] measured calf-liver absorption using the rate of heating technique (0.5–7 MHz) generating the power-law curve fit $\alpha/f = 0.026\ f^{0.17}$. Their data are 14-percent lower than ours at low frequencies, with greater differences at higher frequencies.

C. Pig Liver

Pig liver presents an interesting model for ultrasonic properties (particularly scattering) because its unique structure. The basic composition of the pig liver is different from beef or human liver in that each lobule, the functional unit of the liver, is surrounded by a thin hexagonal layer of collagen [16]. More scattering should therefore be produced because of the multiple impedance mismatches between collagen layers and lobules. Fig. 7 shows the summary of pig-liver attenuation ($\alpha/f = 0.034\ f^{0.32}$) and absorption ($\alpha/f = 0.032\ f^{0.30}$) data. These

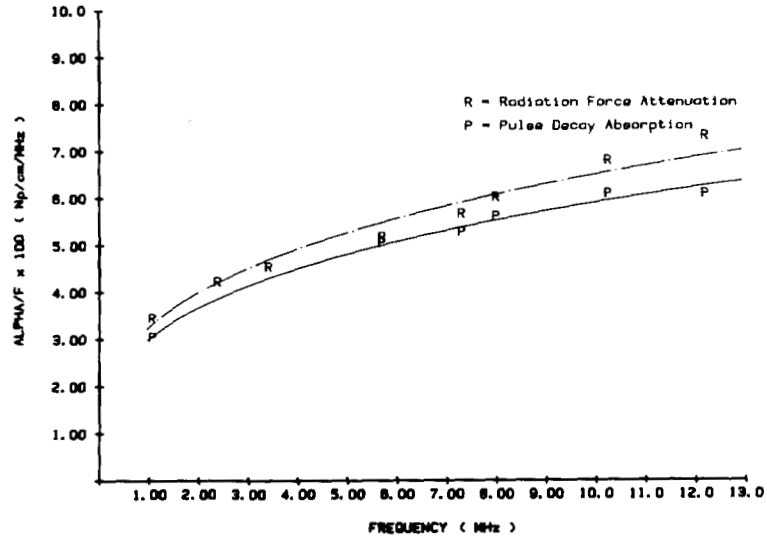

Fig. 6. Absorption (P) and attenuation (A) coefficients for calf liver, with power law curve fits.

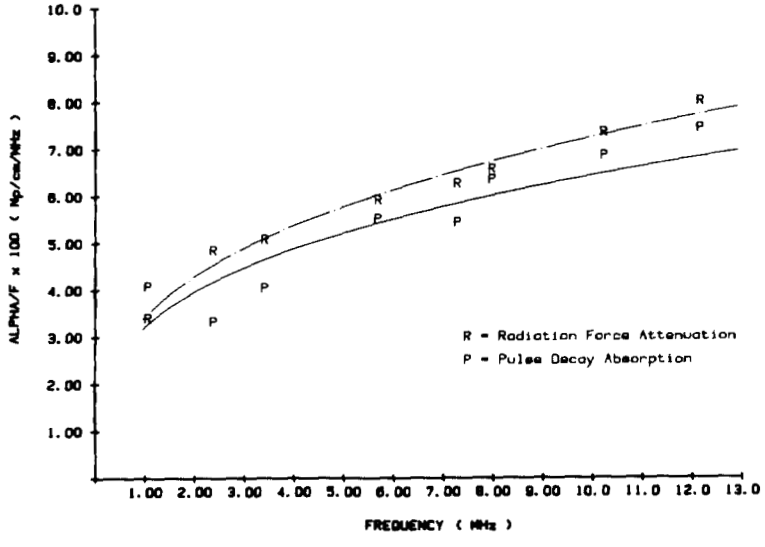

Fig. 7. Absorption (P) and attenuation (A) data for highly collagenous pig liver, with power law curve fits.

data are based on a smaller sample size (sections from two whole livers) as compared to calf liver. Still, some interesting observations can be made. Comparing pig and calf liver absorptions, one finds little difference in magnitude or frequency dependence of the coefficients. Goss *et al.* [6] compared pig liver absorption to that of beef, cat, and mouse livers, finding no significant differences. This agrees with our pig–calf liver comparison, although our values are consistantly higher.

D. Bovine Brain

The brain is composed of two types of tissue, white and grey matter. Since they are structurally different it is desirable to study them independently. It is relatively easy to isolate white matter, but soft grey matter is difficult to remove without mechanical damage. Therefore, in this research, only pulse-decay absorption (which can utilize small sample volumes) was measured for isolated grey and white matter. Attenuation measurements, which require 30 cc or more of tissue, utilized mixed grey–white sections. Fig. 8 summarizes the experiments performed on two samples each of brain tissues.

The data reveal that white brain absorption ($\alpha/f = 0.064\, f^{0.27}$) is considerably higher than that of grey brain ($\alpha/f = 0.012\, f^{0.21}$). This difference most likely arises from compositional differences of the two tissues. White brain is composed of nerve tissues (like grey matter) that are surrounded by myelin (fatty tissue) sheaths. The high lipid concentration in the white tissue is likely to cause increased attenuation. Another difference between the two tissues is the dry weight of white brain is approximately 1.9 times that of grey brain [18]. Fig. 8 also contains a curve for radiation force attenuation of white + grey mixture ($\alpha/f = 0.040\, f^{0.17}$). This curve is positioned be-

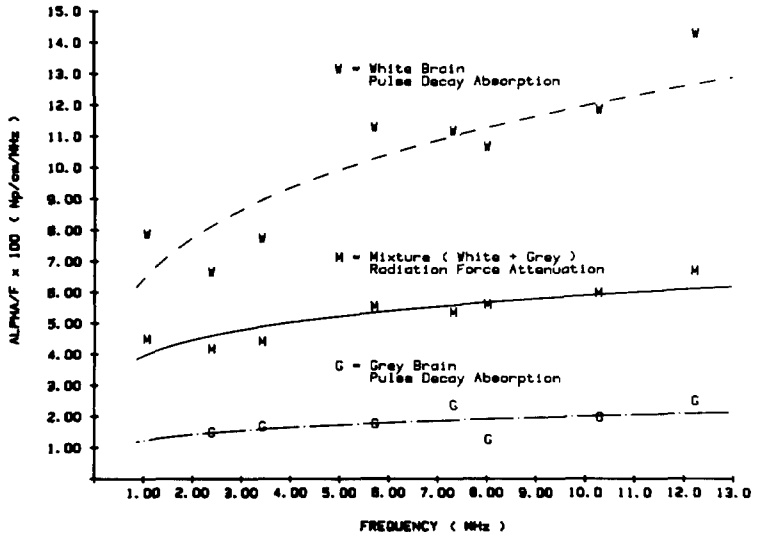

Fig. 8. Absorption of bovine white brain matter (W) and grey brain matter (G), compared with attenuation of mixed white and grey samples (M).

tween the two absorption curves, precisely where the absorption of a 40–60 percent white–grey composite mixture would fall.

Kremkau *et al.* [18] have performed experiments on brain reporting phase-sensitive attenuation values near 0.80 Np/cm MHz for mixed grey-white matter, with phase insensitive measurements approximately 17-percent lower, or 0.066 Np/cm · MHz. These values are higher than ours, but the comparison is reasonable given the differences in technique and likely variability in percent mix of grey and white matter in sections taken from different anatomical locations.

E. Bovine Skeletal Muscle

Sections of beef hind leg muscle were taken from the region 5–20 cm above the termination of the Achilles tendon. Samples were taken between facial planes, with thick collagen bundling surgically removed. Attempts were made to determine attenuation and absorption along and across muscle fibers, to address the effects of anisotropy.

Absorption and attenuation experiments were performed on numerous samples (>15). The results of these experiments proved to be contradictory. Figs. 9(a)–(c) summarize the data collected on three different samples. In all three cases the muscle fibers were believed to run parallel to the axis of insonation. Examination of these graphs shows different results, both in absolute value of attenuation and absorption and in the degree to which absorption contributes to attenuation, including an impossible result, in Fig. 9(a), where absorption is greater than attenuation. To determine the source of variability, several samples were dissected. The fiber orientation of a given sample was found to be variable over centimeter distances. Fig. 10 illustrates this point. If absorption is higher in parallel fiber orientation, then when a thermocouple junction is located in an area of the sample where the fibers are parallel; but if most of the fibers are perpendicular, the measured absorption could be higher than attenuation. It is possible that other skeletal muscles, such as abdominal muscles, have longer and more regular fiber orientations and therefore are better suited to these experiments.

IV. Discussion

Table I is a summary of the tissue absorption and attenuation data collected in this study. The muscle data are excluded due to the uncertainty of our procedures and results.

One key question to address is the influence of scattering on total attenuation. Fig. 11 presents the difference between attenuation and absorption: (attenuation–absorption)/attenuation $\times$ 100 percent as the percent contribution of "scattering." Data shown use the power law fits of attenuation and absorption versus frequency, for calf liver, pig liver, and phantom. At first glance, one might conclude simply that scattering contributes 6–10-percent in pig and calf liver, especially when compared against the convincing phantom data. However, additional considerations warrant discussion.

a) The calf-liver percent difference between absorption and attenuation is nearly constant with frequency. If the difference were truly due to scattering, then scattering would have to increase as $f^{1.2}$, a lower frequency dependence than has been reported by others [2], [19]. This feature implicates some frequency-independent bias, such as a multiplicative constant, as the source of discrepancy between these absorption and attenuation coefficients.
b) Errors in absorption coefficient measurements [1] alone are estimated at 10-percent; however, the use

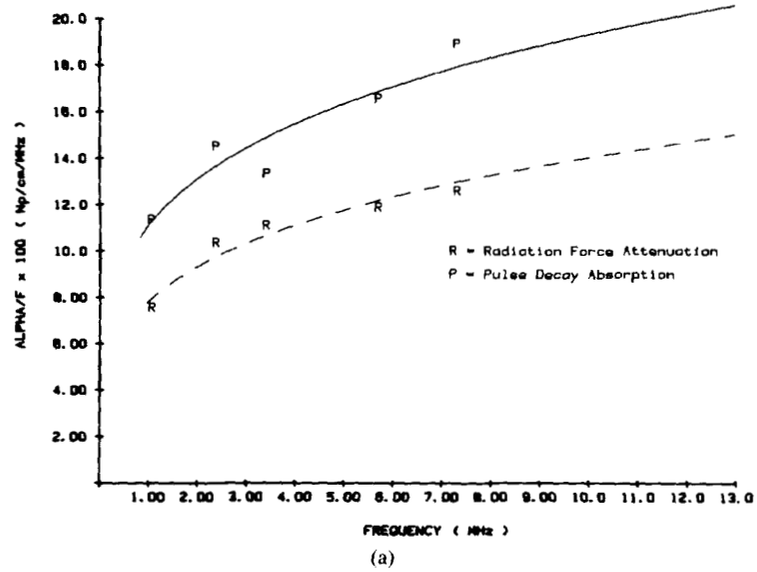

(a)

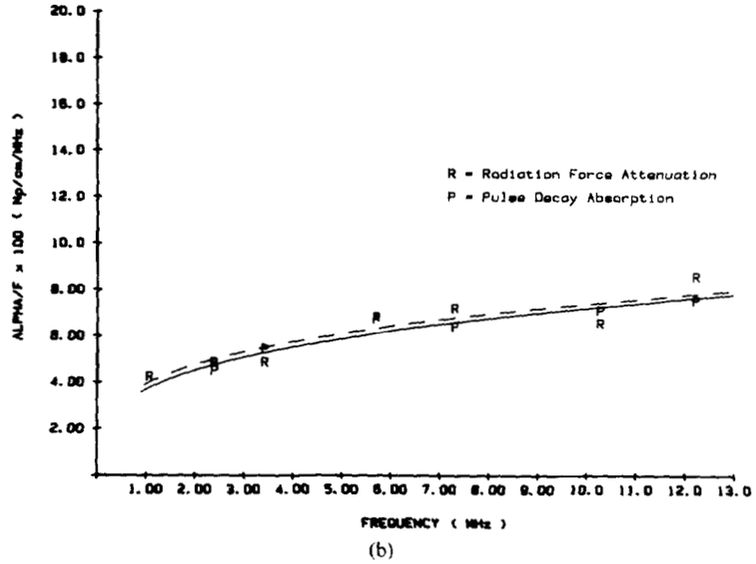

(b)

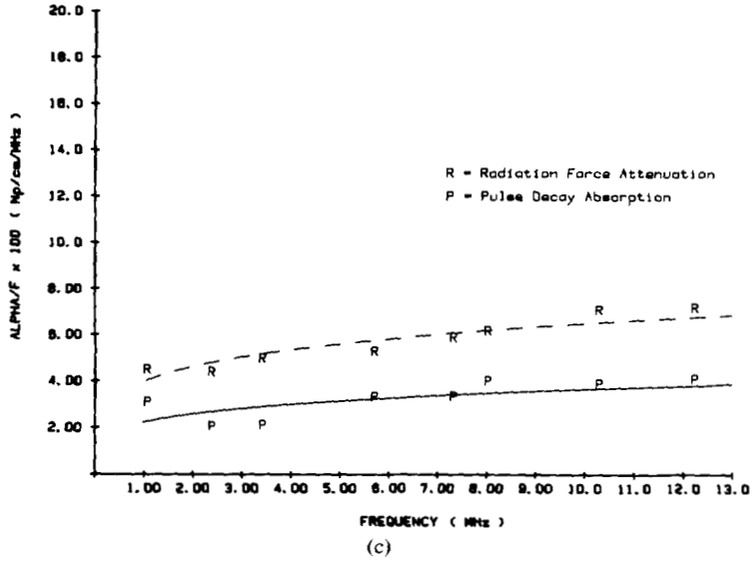

(c)

Fig. 9. Three conflicting cases of absorption (P) and attenuation (A) for bovine skeletal leg muscle, with nominally parallel orientation of beam and muscle fibers.

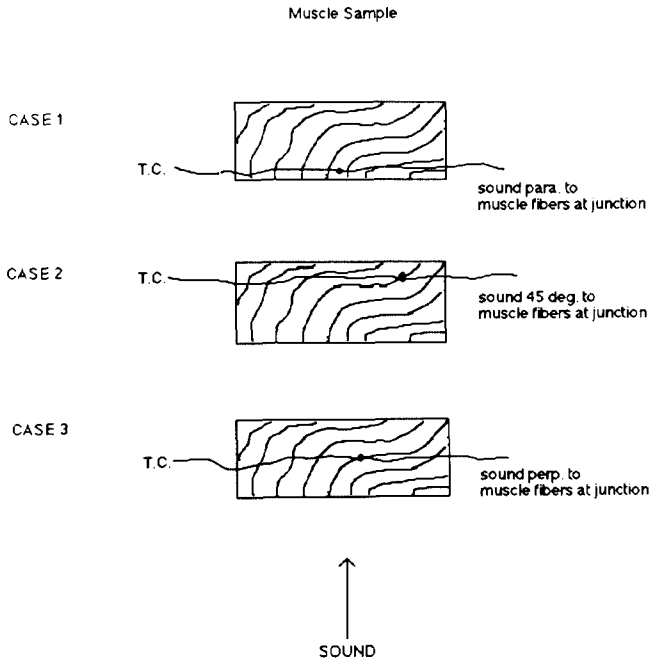

Fig. 10. Possible explanation for discrepencies between absorption and attenuation in muscle, based on highly variable muscle fiber thermocouple orientations.

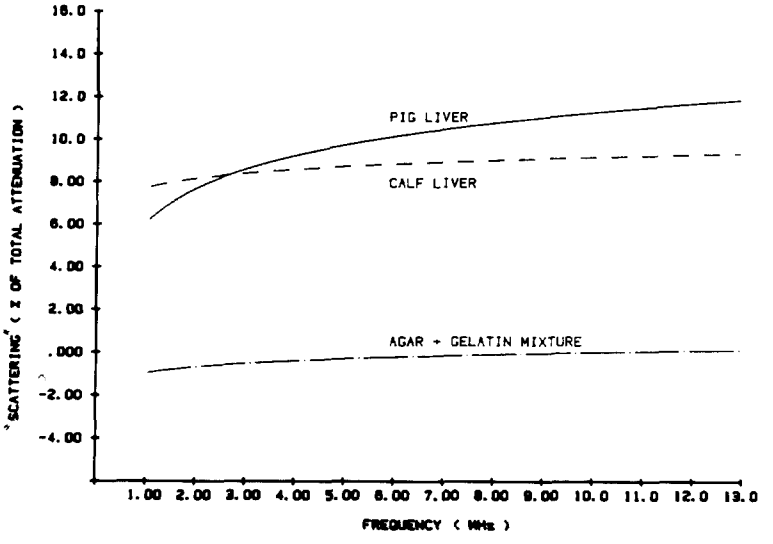

Fig. 11. Ratio of absorption to attenuation, expressed in percent. Data could indicate contribution of scattering in pig and calf liver, but other factors may contribute to measured difference between absorption and attenuation in these cases (see text).

of incorrect tissue density and specific heat values would bias the absorption (but not attenuation) as a frequency-independent constant, moving the percent difference curves of Fig. 11 up or down. One difference between the phantom and liver data is that the tissue contains 2–2.5 times the solid content of the phantom. Thus our use of water density and specific heat values may be valid for the phantom but inappropriate for liver. This major uncertainty can only be resolved by improved thermal–mechanical property measurements.

c) Another consideration involves the comparison between calf and pig liver, where the latter tissue should show enhanced scattering effects from the collagenous lobular structure. However, measurements of absorption and attenuation fail to detect major differences between calf- and pig-liver coefficients. This suggests that something other than scattering may contribute to the measurement bias between attenuation and absorption coefficients.

d) Related experiments by Campbell and Waag directly measured total scattered power in calf liver, concluding that scattering contributed 2-percent ± 2-percent to total attenuation [2]. Also, our homog-

enization experiments [17], [18] failed to duplicate the results of Pauly and Schwan [3], instead finding essentially no difference between whole and homogenized liver attenuation.

Considering the above arguments it is likely that the percent difference between attenuation and absorption in livers, as reported in Fig. 11, is caused by less than 4-percent true scattering, with at least 5–6 percent bias in absorption caused by use of incorrect values of density and specific heat.

V. Conclusion

It is possible to compare tissue attenuation and absorption coefficients using phase-insensitive insertion loss and pulse decay measurements. The latter method has higher uncertainty [1] (approximately 10 percent), depending on material properties such as specific heat, which are difficult to estimate accurately. Results on calf and pig liver show that scattering contributes less than 10 percent to total attenuation. Data from bovine grey, white, and mixed brain tissue support the postulate that absorption dominates attenuation. Bovine skeletal muscle posed additional problems due to the strong tissue anisotropy, where the beam–fiber orientation appeared to contribute the largest variability to differences between attenuation and absorption.

Considering these data and other recent results from Rochester [2], [13], [14], [17] the weight of evidence points to absorption as the dominant loss mechanism, with scattering (intensity) cross sections for liver and brain limited to 5×10^{-3} $(\text{cm} \cdot \text{MHz})^{-1}$ or less in the 1–12 MHz frequency range. These results should enable better understanding of the underlying mechanisms of tissue–ultrasound interaction, with corresponding improvements in modeling and medical applications.

References

[1] K. J. Parker and M. E. Lyons, "Absorption and attenuation in soft tissues I—Calibrations and error analysis," *IEEE Trans. Ultrason. Ferroelec. Freq. Control*, vol.35, no. 2, pp. 242-252, Mar. 1988.

[2] J. A. Campbell and R. C. Waag, "Measurement of calf liver ultrasonic differential and total scattering cross sections," *J. Acoust. Soc. Amer.*, vol. 75, no. 2, pp. 603-611, 1984.

[3] H. Pauly and H. P. Schwan, "Mechanisms of absorption of ultrasound in liver tissues," *J. Acoust. Soc. Amer.*, vol. 50, no. 2, pp. 692-699, 1971.

[4] S. A. Goss, R. L. Johnston, and F. Dunn, "Comprehensive compilation of empirical ultrasonic properties of mammalian tissue," *J. Acoust. Soc. Amer.*, vol. 64, no. 2, pp. 423-457, 1978.

[5] ——, "Compilation of empirical ultrasonic properties, II," *J. Acoust. Soc. Amer.*, vol. 68, no. 1, pp. 93-108, 1980.

[6] S. A. Goss, L. A. Frizzell, and F. Dunn, "Ultrasonic absorption and attenuation in mammalian tissues," *Ultrasound Med. Biol.*, vol. 5, pp. 181-186, 1979.

[7] D. K. Nassiri and R. C. Hill, "The differential and total bulk acoustic scattering cross sections of some human and animal tissues," *J. Acoust. Soc. Amer.*, vol. 79, no. 6, pp. 2034-2046, 1986.

[8] P. W. Marcus and E. L. Carstensen, "Problems with absorption measurements of inhomogeneous solids," *J. Acoust. Soc. Amer.*, vol. 58, no. 6, pp. 1334-35, 1975.

[9] L. A. Frizzell, E. L. Carstensen, and J. D. Davis, "Ultrasonic absorption in liver tissue," *J. Acoust. Soc. Amer.*, vol. 65, no. 5, pp. 1309-1312, 1979.

[10] S. A. Goss, J. W. Cobb, and L. A. Frizzell, "Effect of beamwidth and thermcouple size on the measurement of ultrasonic absorption using the thermoelectric technique, in *Proc. IEEE Ultrason. Symp.*, 1977, pp. 206-211.

[11] K. J. Parker, "The thermal pulse decay technique for measuring ultrasonic absorption coefficients," *J. Acoust. Soc. Amer.*, vol. 74, no. 5, pp. 1356-1361, 1983.

[12] ——, "Effects of heat conduction and sample size on the ultrasonic absorption measurement," *J. Acoust. Soc. Amer.*, vol. 77, no. 2, pp. 719-725, 1985.

[13] K. J. Parker, "Ultrasonic attenuation and absorption in liver tissue," *Ultrasound Med. Biol.*, vol 9, no. 4, pp. 363-369, 1983.

[14] K. J. Parker and R. C. Chivers, "On liver homogenization experiments," submitted to *IEEE Trans. Ultrason. Ferroelec. Freq. Control.*

[15] F. Dunn *et al.*, "Elements of tissue characterization I, Ultrasonic propagation properties," in *Ultrasonic Tissue Characterization II*, M. Linzer, Ed. U.S. Dept. Commerce, NBS Special Publication 525, Washington, DC, 1979, 19-38.

[16] J. Bloom and H. Fawcett, *A Textbook of Histology, 9th Edition*. New York: W. B. Saunders, 1968, Chapt. 27.

[17] M. E. Lyons, R. C. Chivers, and K. J. Parker, "Absorption dominates attenuation in soft tissues," in *Proc. IEEE Ultrason. Symp.* 1986, pp. 871-873.

[18] F. W. Kremkau, R. W. Barnes, and C. P. McGraw, "Ultrasonic attenuation and propagation speed in normal human brain," *J. Acoust. Soc. Amer.*, vol. 70, no. 1, pp. 29-38, 1981.

Mark E. Lyons for a biography and photograph, please see page 252 of the March issue of this TRANSACTIONS.

Kevin J. Parker (S'79-M'81-SM'87) for a biography and photograph, please see page 252 of the March issue of this TRANSACTIONS.